iJRASET
International Journal For Research in Applied Science and Engineering Technology

INTERNATIONAL JOURNAL FOR RESEARCH

IN APPLIED SCIENCE & ENGINEERING TECHNOLOGY

Volume: 14 **Issue:** III **Month of publication:** March 2026

DOI: https://doi.org/10.22214/ijraset.2026.79153

www.ijraset.com

Call: 08813907089 | E-mail ID: ijraset@gmail.com

International Journal for Research in Applied Science & Engineering Technology (IJRASET)
ISSN: 2321-9653; IC Value: 45.98; SJ Impact Factor: 7.538
Volume 14 Issue III Mar 2026- Available at www.ijraset.com

Green Synthesis of Titanium Dioxide Nanoparticles Using *Chamaecostus Cuspidatus* Leaf Extract

Kavitha R[1], Dr. J. Antony Rajam[2]
[1]*PG Department of Chemistry (SSC), St. Mary's College (Autonomous) (Affiliated to Manonmaniam Sundaranar University), Thoothukudi, 628001, Tamil Nadu, India*
[2]*Assistant Professor, PG Department of Chemistry (SSC), St. Mary's College (Autonomous) (Affiliated to Manonmaniam Sundaranar University), Thoothukudi, 628001, Tamil Nadu, India.*

Abstract: ***Green synthesis of nanoparticles using plant extracts is an eco-friendly and sustainable method. In this study, titanium dioxide (TiO_2) nanoparticles were synthesized using Chamaecostus cuspidatus leaf extract as a reducing and stabilizing agent, with titanium isopropoxide as the precursor. The nanoparticles were characterized using UV–Visible spectroscopy, FT-IR, XRD, FE-SEM, EDAX and TGA to study their optical, structural, morphological, elemental and thermal properties. The results confirmed the formation of anatase phase TiO_2 nanoparticles with an average crystallite size of 12.10 nm. FE-SEM analysis showed quasi-spherical particles with slight agglomeration and EDAX confirmed the presence of titanium and oxygen. The nanoparticles exhibited good thermal stability. In addition, they showed antibacterial activity, anticorrosion performance and improved shelf-life under ambient conditions. These findings suggest that the synthesized nanoparticles have potential applications in medical, environmental and agricultural fields.***

Keywords: Green synthesis, TiO_2 nanoparticles, Chamaecostus cuspidatus, Antibacterial activity, Anticorrosion activity

I. INTRODUCTION

Green synthesis of nanoparticles using plant extracts has emerged as an eco-friendly, cost-effective, and sustainable alternative to conventional chemical and physical methods [1]. Among various metal oxides, titanium dioxide (TiO_2) nanoparticles have attracted significant attention due to their excellent optical, photocatalytic, antibacterial, and anticorrosion properties [2]. However, traditional synthesis methods often involve toxic chemicals, high energy consumption, and environmental risks, which limit their large-scale applications [3]. In recent years, plant-mediated synthesis has gained importance as plant extracts contain bioactive compounds such as flavonoids, phenols, and terpenoids that act as natural reducing and stabilizing agents. *Chamaecostus cuspidatus*, commonly known as the insulin plant, is rich in such phytochemicals and possesses notable medicinal properties, including antioxidant, anti-inflammatory, and antimicrobial activities [4]. In this study, TiO_2 nanoparticles were synthesized using *Chamaecostus cuspidatus* leaf extract through a green synthesis approach. The synthesized nanoparticles were characterized and evaluated for their antibacterial, anticorrosion, and shelf-life extension applications, highlighting their potential in environmental, biomedical, and agricultural fields.

II. LITERATURE REVIEW

[1] Sakshi Sikaria et al., (2026) studied on "*Vitex negundo* leaf extract-assisted synthesis of TiO_2 nanoparticles and deciphering its *in vitro* antibacterial, antibiofilm, cytotoxic and anti-migratory activities" and reported that Biogenic TiO_2 nanoparticles were synthesized using *Vitex negundo* leaf extract and characterized for their properties and bioactivities. The nanoparticles showed a band gap of 3.25 eV, crystalline structure and ~50 nm hexagonal morphology. They exhibited strong antibacterial and antibiofilm activity, along with cytotoxic effects against oral carcinoma cells (IC_{50} = 68.82 µg/mL) and inhibition of cell migration, indicating anti-metastatic potential [5].

[2] Abouelkacem Sahraoui et al., (2025) studied on "Synthesized TiO_2 nanoparticles using *Eucalyptus globulus* leaf extract" and reported that titanium butoxide was used as a precursor under mild thermal treatment to obtain four biosynthesized samples via single- and double-thermal treatments. Characterization by DRS, FT-IR, Raman, XRD, UV–Visible and SEM-EDX revealed uniform spherical morphology, predominant anatase phase and confirmed the role of phenolic and flavonoid acids in Ti^{4+} reduction. The double-thermal-treated sample showed properties closest to commercial TiO_2, demonstrating an eco-friendly method for producing high-quality nanoparticles with desirable physicochemical characteristics [6].

[3] Khrsheed Ahmed et al., (2025) studied on "Highly precise electrochemical biosensing of urea through *Trigonella foenum-graecum* leaf extract mediated green synthesis of titanium dioxide nanoparticles" and reported that TiO_2 nanoparticles were synthesized using *Trigonella foenum-graecum* leaf extract and applied in a urease-based electrochemical biosensor for urea detection. The biosensor showed high sensitivity with a detection limit of 2.28×10^{-2} µM, fast response time (35 s), good stability (60 days) and reusability (13 cycles). It was successfully used for urea detection in blood and environmental samples [7].

[4] Aminur Rahman et al., (2025) studied on "Green synthesis of antibacterial TiO_2 nanoparticles using citrus lemon extract to combat MDR *Clostridium perfringens"* and reported that TiO_2 nanoparticles (TiO_2-NPs) were synthesized using Titanium (IV) oxide solution and citrus lemon extract as reducing and capping agent. UV–Vis confirmed formation (λmax 315 nm), while AFM, SEM and TEM showed particles ~37.5 nm long and 12.3 nm wide. FTIR and XRD verified bond formation and crystallinity. Antibacterial assays showed strong inhibition (27 ± 0.5 mm) against MDR *Clostridium perfringens*, with MIC and MBC values of 5 and 10 µg/ml. MTT assay confirmed biocompatibility at 5 µg doses. The synthesized TiO_2-NPs were recommended as eco-friendly antibacterial agents and sanitizers for farm and household waste environments [8].

[5] Shinta Eryamana Putri et al., (2025) studied on "Effect of *Elaeis guineensis Jacq.* Leaf extracts concentration in the optical, structure, morphology analysis of titanium dioxide nanoparticles" and reported that The effect of *Elaeis guineensis* leaf extract on TiO_2 nanoparticle synthesis was investigated. The results showed that extract concentration influenced phase formation, with anatase dominant at 20%, while rutile and brookite appeared at other concentrations. An increase in bandgap and a morphological shift from needle-like to rod-like structures were observed, and EDX confirmed the presence of titanium and oxygen, indicating its suitability as a sustainable synthesis agent [9].

III. MATERIALS AND METHODS

A. Green Synthesis of Titanium dioxide nanoparticle using Chamaecostus cuspidatus leaf extract

1) Materials Used

The green synthesis of titanium dioxide nanoparticles using *Chamaecostus cuspidatus* leaf extract was carried out using materials such as *Chamaecostus cuspidatus* leaves, titanium isopropoxide, isopropyl alcohol, a magnetic stirrer, a centrifugating machine, a hot air oven and a muffle furnace.

2) Preparation of Leaf Extract

The leaves were separated from the plant, thoroughly washed with double distilled water to remove surface impurities and dried in the dark at room temperature for approximately 15 days. The leaves were smashed into a coarse powder using a blender. The leaf powder was stored in a dry, airtight container away from direct sunlight. About 5 g of dry powder was added in 100 mL of double distilled water and kept in a magnetic stirrer for 45 minutes. The herbal extraction was cooled to 37°C before being filtered multiple times to remove any remaining waste or debris. Furthermore, all unconsolidated components were removed from the plant extract by centrifugation at 5000 rpm for 10 minutes and the resultant extract was kept at 4°C for future use.

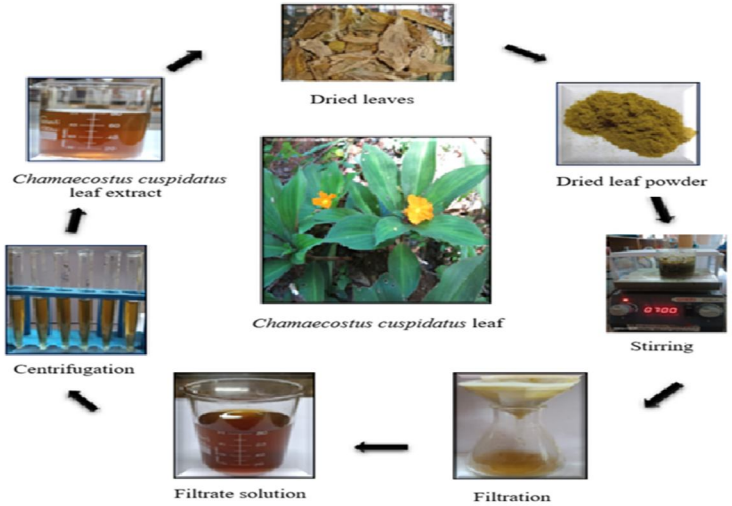

Fig. 3.1 Schematic representation of the Preparation of Leaf extract

3) Synthesis of Titanium dioxide Nanoparticles

The *Chamaecostus cuspidatus* treated TiO_2 nanoparticles were synthesized by dissolving 5 mL of titanium (IV) isopropoxide ($Ti[OCH(CH_3)_2]_4$) in 50 mL of isopropyl alcohol, followed by the addition of 25 mL of *Chamaecostus cuspidatus* leaf extract under constant stirring at 50°C for 2 hours. The resulting gel-like mixture was aged for 24 hours. The obtained brownish-green gel was then transferred to a hot air oven and kept at 80°C for 8 hours. The dried powder was further calcined at 350°C for 5 hours. Finally, the product was finely ground and stored for further analysis. The synthesized nanoparticles prepared using *Chamaecostus cuspidatus* leaf extract were designated as TiO_2 – C throughout the study.

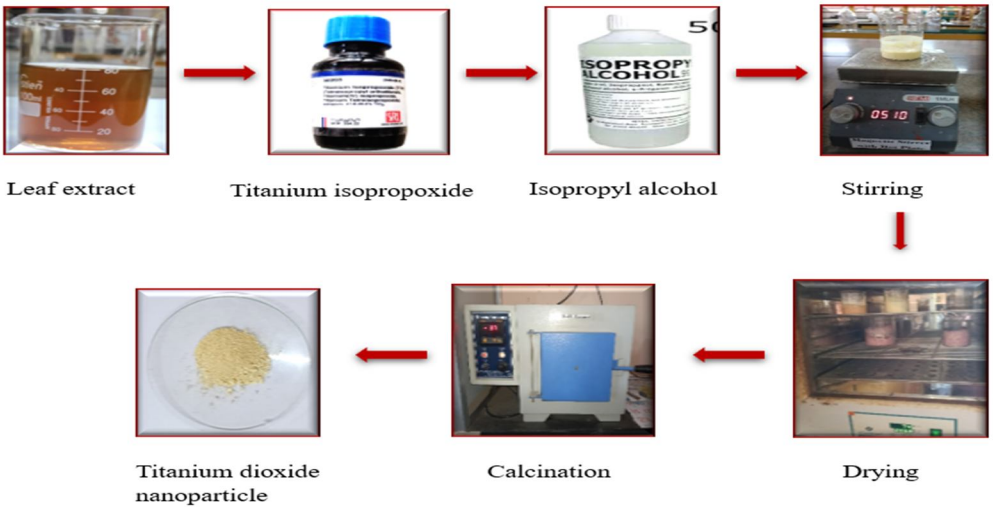

Fig. 3.2 Schematic representation of the Synthesis of TiO_2 Nanoparticles

IV. RESULTS AND DISCUSSION

A. Characterizations of TiO_2 Nanoparticles

1) UV – Visible Spectroscopy

The UV–Visible absorption spectrum of the green-synthesized TiO_2 – C nanoparticles using *Chamaecostus cuspidatus* leaf extract is shown (Fig. 4.1) with absorption in the range of 200 – 900 nm.

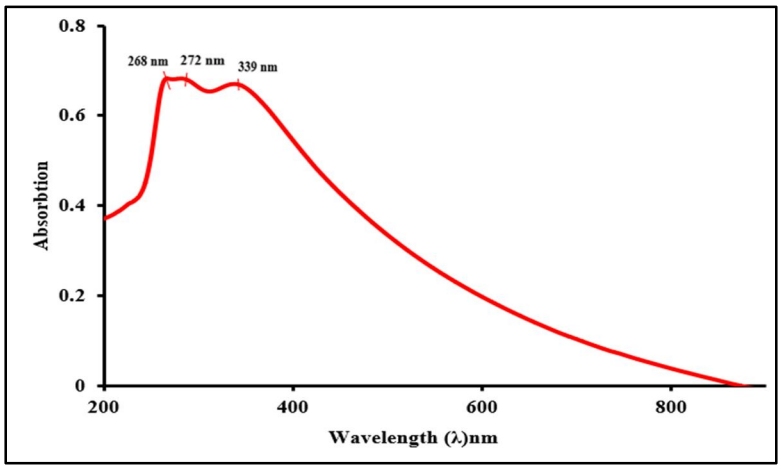

Fig. 4.1 UV- Visible absorption spectrum of TiO_2 – C Nanoparticles

A strong absorption peak is observed at 268 nm, confirming the formation of TiO_2 – C nanoparticles. Minor peaks at 272 nm and 339 nm may be due to surface functional groups from the leaf extract. The absorbance decreases gradually toward the visible region with very low absorption beyond 400 nm, indicating good purity of the nanoparticles. The slight blue shift suggests the formation of small-sized nanoparticles due to quantum confinement effects. Similar UV absorption peaks in the range of 260 – 300 nm have been reported for plant-mediated TiO_2 nanoparticles in previous studies [10]. These results confirm the successful green synthesis of TiO_2 – C nanoparticles.

2) Fourier Transform - Infrared Spectroscopy

The FT-IR spectrum of the green-synthesized TiO_2 – C nanoparticle is shown (Fig. 4.2). A broad absorption band observed at 3358.9 cm^{-1} is attributed to O–H stretching vibrations of surface hydroxyl groups and adsorbed moisture, which is commonly observed in green synthesized TiO_2 nanoparticles [11]. The absorption bands at 2924.2 cm^{-1} and 2854.3 cm^{-1} correspond to C–H stretching vibrations, indicating the presence of organic compounds acting as reducing and stabilizing agents during green synthesis. The peak observed at 1634.8 cm^{-1} is assigned to C=O stretching and H–O–H bending vibrations, suggesting the involvement of biomolecules in nanoparticle formation [12]. The absorption bands at 1456.7 cm^{-1} and 1384.5 cm^{-1} correspond to C–N/C–O stretching vibrations, while the peaks at 1103.6 cm^{-1} and 1046.2 cm^{-1} are attributed to C–O stretching vibrations, indicating the presence of organic functional groups on the nanoparticle surface. The strong absorption bands observed at 602.4 cm^{-1}, 486.1 cm^{-1} and 451.3 cm^{-1} are assigned to Ti–O–Ti and Ti–O lattice vibrations, confirming the formation of TiO_2 – C nanoparticles, which is consistent with previously reported TiO_2 nanoparticle studies [10]. Overall, the FTIR results confirm the successful green synthesis and stabilization of TiO_2 – C nanoparticles.

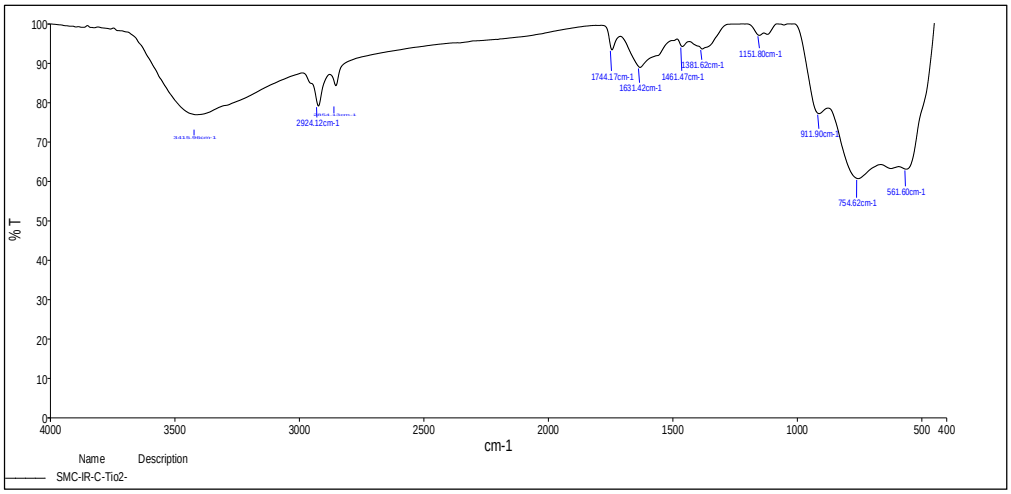

Fig. 4.2 FT-IR Spectrum of TiO_2 – C Nanoparticles

3) X-ray Diffraction Analysis

The X-ray diffraction (XRD) analysis of the *Chamaecostus cuspidatus* leaf extract mediated synthesized TiO_2 – C nanoparticles was carried out using Cu Kα radiation (λ = 1.5406 Å) to determine the crystalline phase, structural purity and average crystallite size. The XRD pattern of the TiO_2 – C sample is presented shown (Fig. 4.3). The prominent diffraction peaks observed at 2θ values of 25.6282° and 48.3044° correspond to the interplanar d-spacing values of 3.476 Å and 1.884 Å, respectively. These peaks were indexed to the (101) and (200) crystallographic planes of tetragonal anatase TiO_2 and are in good agreement with the standard JCPDS card No. 96-153-0152, which confirms the formation of crystalline anatase TiO_2. The structural parameters of the anatase phase are consistent with the standard crystallographic data [13].

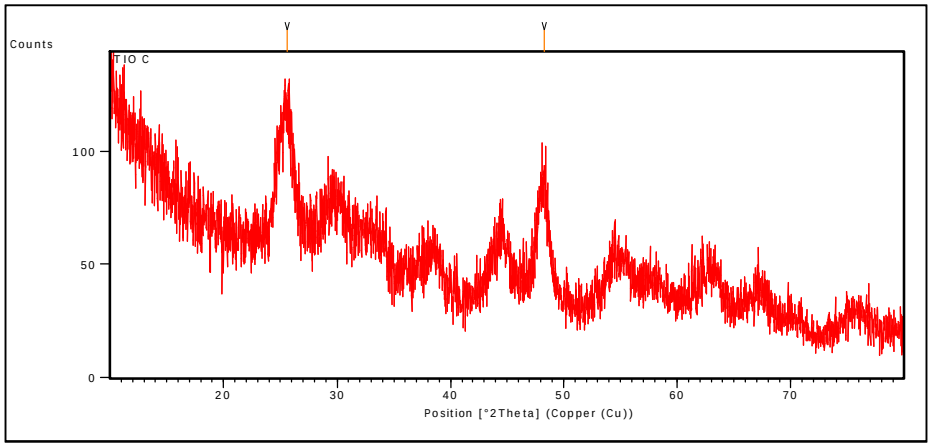

Fig. 4.3 XRD Spectrum of TiO_2 – C Nanoparticles

The obtained TiO_2 belongs to the tetragonal crystal system with lattice parameters, a = 3.7800 Å and c = 9.5100 Å. The absence of any additional diffraction peaks in the pattern indicates that no secondary phases such as rutile or brookite are present, thereby confirming the high phase purity of the synthesized TiO_2 – C sample. Among the observed reflections, the (101) plane exhibits higher intensity, indicating its preferential orientation, which is a characteristic feature of nanocrystalline anatase TiO_2 [14]. Furthermore, the diffraction peaks show noticeable broadening, which is mainly attributed to the small crystallite size of the nanoparticles. The average crystallite size calculated using the Debye–Scherrer equation was found to be 12.10 nm, confirming the nanocrystalline nature of the TiO_2 – C sample. Similar peak broadening due to nanoscale crystallite size has been reported for TiO_2 nanomaterials synthesized by different methods [15]. Thus, the XRD results clearly confirm the successful formation of phase-pure, nanocrystalline anatase TiO_2 with a tetragonal crystal structure for the TiO_2 – C sample.

4) Field Emission-Scanning Electron Microscopy

Field Emission Scanning Electron Microscopy (FE-SEM) was employed to investigate the surface morphology of the synthesized TiO_2 – C composite, as shown (Fig. 4.4). The micrographs reveal the formation of densely packed and agglomerated nanoparticles with nearly spherical to irregular (quasi-spherical) morphology [15]. The particles are uniformly distributed over the surface without noticeable cracks, indicating good structural formation of the synthesized material.

At higher magnification, the surface appears rough and porous, which is beneficial for increasing the active surface area. The particle size measured from different regions lies in the range of ~ 43 – 130 nm with an average particle size of ~ 85 nm, confirming the nanoscale nature of the sample. The observed agglomeration is mainly due to the high surface energy and strong interparticle interactions of the nanoparticles [15]. Overall, the FE-SEM analysis confirms the successful formation of nanostructured material with quasi-spherical nanoparticles assembled into porous clustered structures and uniform surface morphology [16].

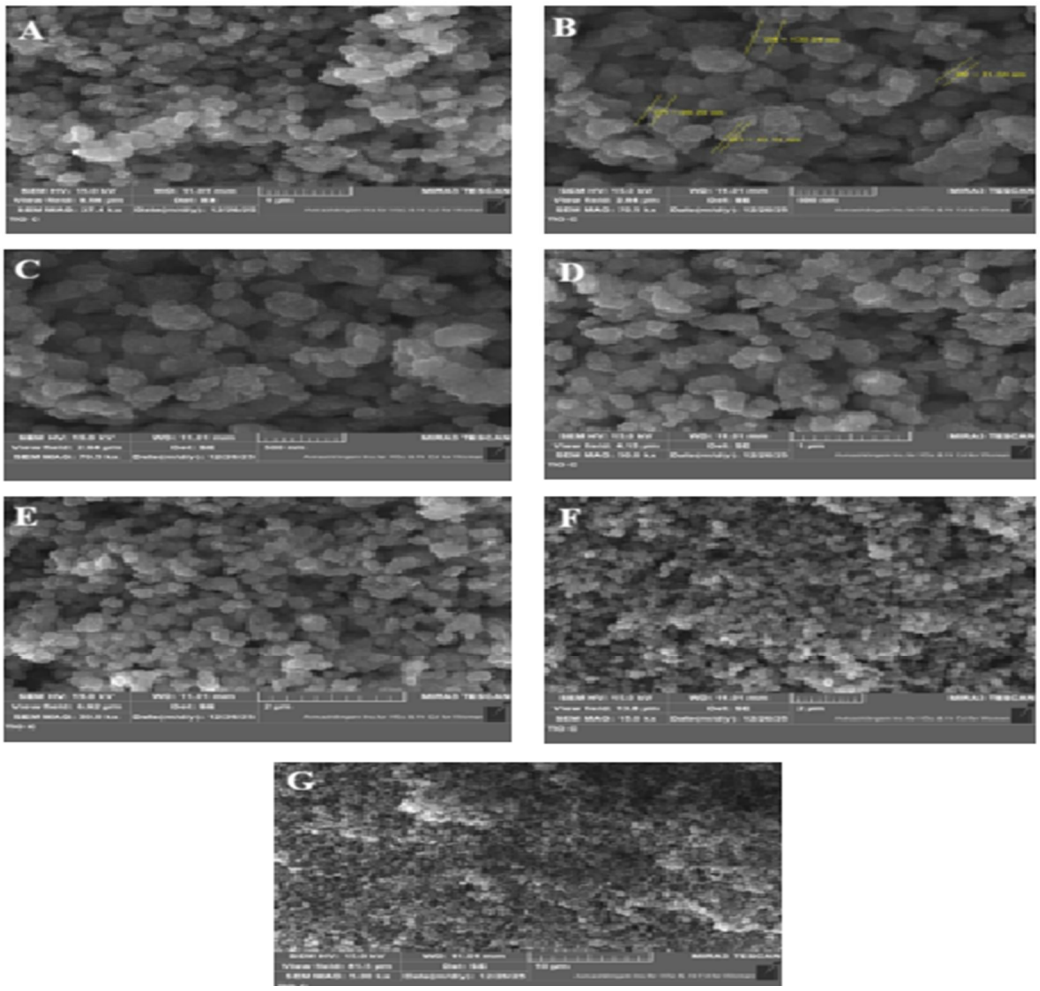

Fig. 4.4 FE-SEM images of TiO_2 – C Nanoparticles

5) Energy Dispersive X-ray Analysis spectroscopy

The Energy Dispersive X-ray (EDAX) spectroscopy image shows the elemental composition and purity of the synthesized TiO_2 – C nanoparticles. The EDAX images of TiO_2 – C nanoparticles are presented in (Fig. 4.5), while the corresponding EDAX spectrum is shown (Fig. 4.6). The spectrum confirms the presence of titanium (Ti) and oxygen (O) as the major elements, along with small amounts of sodium (Na) and potassium (K). The quantitative EDAX results reveal 35.87 wt % oxygen and 56.55 wt % titanium, corresponding to atomic percentages of 60.25 % and 31.72 %, respectively, which are in good agreement with the expected stoichiometric ratio of TiO_2 [15].

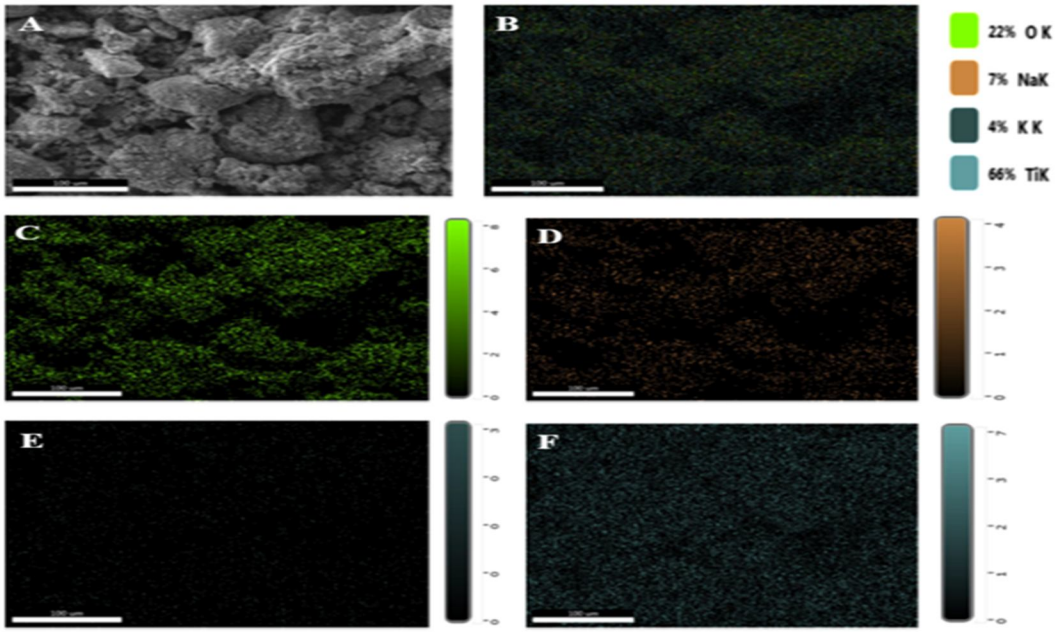

Fig. 4.5 EDAX images of TiO_2 – C Nanoparticles

In addition to these principal elements, Na (5.85 wt %, 6.84 at. %) and K (1.73 wt %, 1.19 at. %) are detected in trace levels. The appearance of these alkali metals is mainly attributed to residual precursor salts, plant-derived phytochemicals, or stabilizing/capping agents used during the green synthesis process, where a small amount of ions may remain adsorbed on the nanoparticle surface even after repeated washing and calcination. In some cases, these ions can also be incorporated into the surface lattice during nanoparticle growth. However, their low concentration indicates that they do not form any secondary phase and only exist as minor surface-associated species. Furthermore, the elemental mapping images show a uniform distribution of Ti and O throughout the analyzed region, confirming the formation of a homogeneous TiO_2 matrix, whereas Na and K are sparsely distributed. Thus, the EDAX analysis confirms the successful formation of TiO_2 nanoparticles with high purity and the detected trace elements originate from the synthesis route rather than from any structural impurity. The quantitative EDAX results are summarized in (Table 4.1).

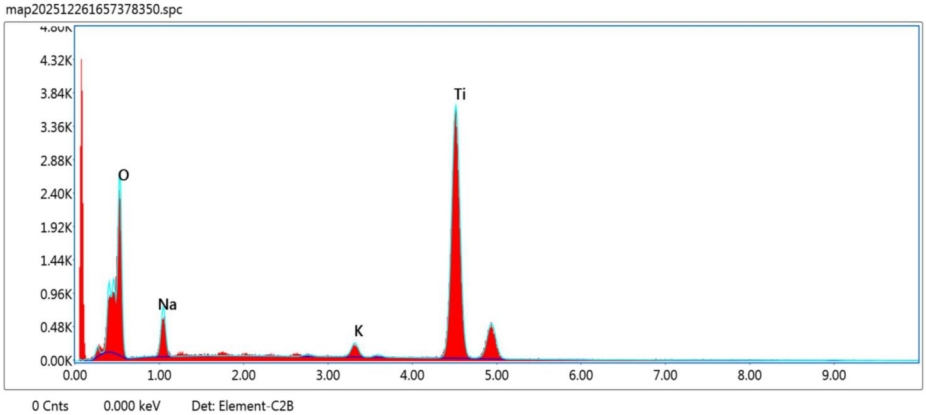

Fig. 4.6 EDAX spectrum of TiO_2 – C Nanoparticles

Table 4.1 EDAX smart quant results of TiO_2 – C

Element	Weight %	Atomic %	Net Intensity	Error %	K-ratio	Z	A	F
O K	35.87	60.25	179.15	10.76	0.0601	1.1535	0.1453	1.0000
Na K	5.85	6.84	59.62	9.77	0.0221	1.0451	0.3612	1.0008
K K	1.73	1.19	25.92	9.23	0.0172	0.9650	0.9813	1.0458
Ti K	56.55	31.72	543.51	2.33	0.5047	0.8886	1.0020	1.0028

6) Thermogravimetric Analysis

The thermogravimetric analysis (TGA) curve of the TiO_2 – C composite is shown (Fig. 4.7). The TGA curve reveals a total weight loss of approximately 10.3 % up to 1000°C, indicating the good thermal stability of the TiO_2 – C composite. The initial weight loss of about 2.7 % below ~250°C is attributed to the removal of physically adsorbed moisture and volatile surface-bound species. The second stage, showing another ~2.7 % loss between ~250–700°C, corresponds to the decomposition of residual organic components and the partial oxidation of carbon present in the composite. The third degradation step of about ~2.9 % from ~700–950°C is associated with the combustion of more stable carbon species and structural rearrangement within the TiO_2 – C framework. After these stages, about 89.7 % of the material remains thermally stable, indicating the strong structural integrity of the TiO_2 – C composite at elevated temperatures. Beyond this temperature, the material exhibits minimal mass loss, suggesting the formation of thermally stable titanium oxide phases [15]. Overall, the low total mass loss and the gradual degradation behaviour confirm that the TiO_2 – C composite possesses high thermal stability, making it suitable for high-temperature applications such as photocatalysis, electrodes and energy storage systems [17].

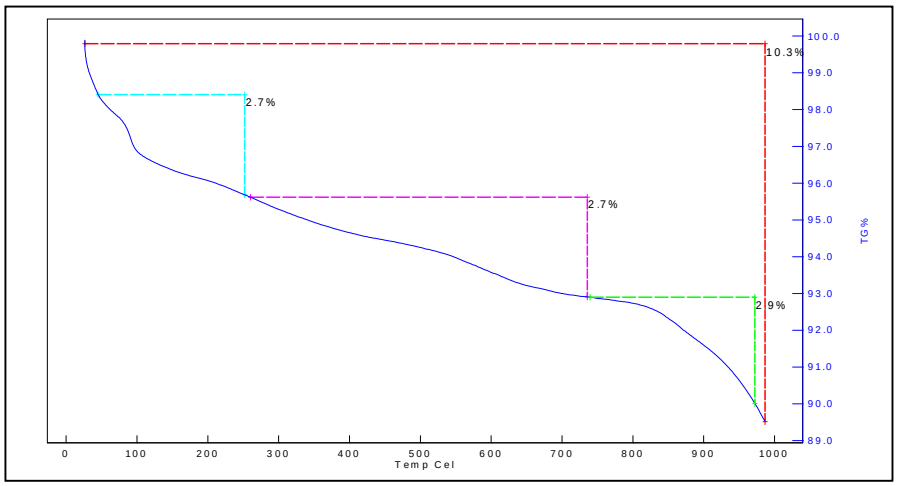

Fig. 4.7 TGA Curve of TiO_2 – C Nanoparticles

7) Combined Spectrum of Thermogravimetric (TG), Derivative Thermogravimetric (DTG) and Differential Thermal Analysis (DTA)

The TG, DTG and DTA curves of the synthesized TiO_2 nanoparticles are shown (Fig. 4.8). The thermogravimetric (TG) curve shows a gradual mass loss from room temperature to about 950°C. The initial weight loss below ~ 150°C is attributed to the removal of physically adsorbed moisture and volatile impurities present on the surface of the material. A continuous mass reduction observed between ~ 150 – 800°C corresponds to the decomposition of residual organic components and precursor species. Above ~ 800°C, the mass loss becomes very small, indicating the formation of a thermally stable inorganic titanium oxide phase.

The derivative thermogravimetric (DTG) curve exhibits a sharp peak in the low-temperature region, confirming rapid dehydration and removal of volatile species [18]. A broad DTG region between ~ 200 – 700°C represents the main degradation stage due to the decomposition of organic moieties and structural rearrangements. A small DTG variation at higher temperatures (~ 800 – 900°C) suggests slow structural stabilization of the material.

The differential thermal analysis (DTA) curve shows a broad endothermic region below ~ 200°C corresponding to moisture evaporation. A wide thermal peak around ~ 300 –500°C is attributed to decomposition of organic components and phase transformation. At higher temperatures, the smooth DTA profile indicates stabilization of the inorganic framework [16]. Overall, the

TG – DTG – DTA results confirm that the synthesized TiO_2 – C material possesses good thermal stability and is suitable for high-temperature applications.

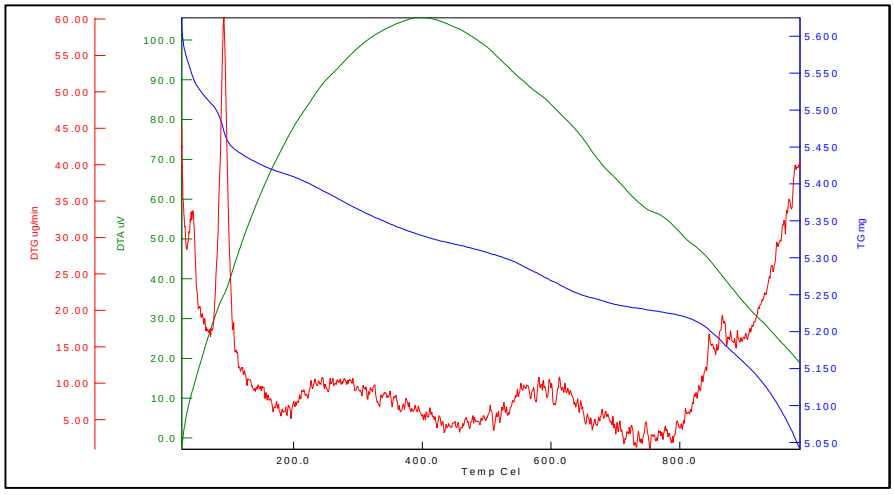

Fig. 4.8 TG – DTG – DTA Curve of TiO_2 – C Nanoparticles

B. Applications

1) Antibacterial Activity

The antibacterial activity of TiO_2–C nanoparticles was evaluated against *Escherichia coli*, *Staphylococcus aureus*, *Bacillus subtilis*, *Bacillus cereus* and *Klebsiella pneumoniae* using the disc diffusion method [19], with ciprofloxacin as the standard antibiotic. The inhibition zones for TiO_2–C ranged from 8 to 9 mm, whereas ciprofloxacin showed higher activity (22–30 mm) against all tested strains (Table 4.2; Fig. 4.9). TiO_2–C exhibited inhibition zones of 8 mm against *E. coli*, *Bacillus subtilis* and *Klebsiella pneumoniae* and 9 mm against *Staphylococcus aureus* and *Bacillus cereus*. The nanoparticles showed comparatively higher activity against Gram-positive bacteria than Gram-negative bacteria, likely due to differences in cell wall structure. Overall, TiO_2–C nanoparticles demonstrated moderate antibacterial activity, indicating their potential as an alternative antimicrobial agent.

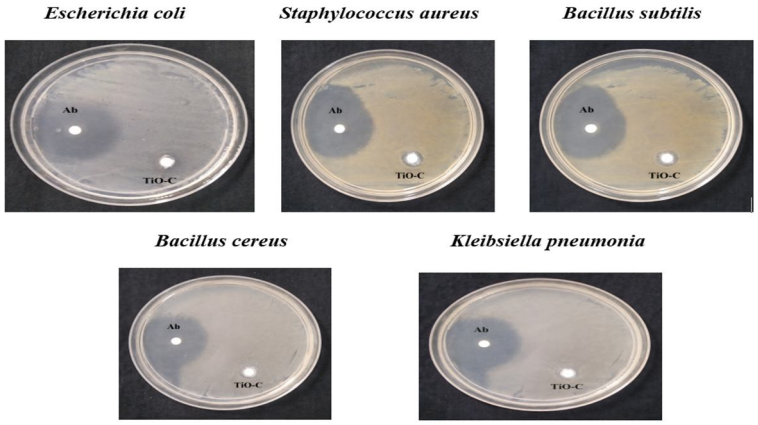

Fig. 4.9 Antibacterial activity image of TiO_2 Nanoparticles

Table 4.2 Antibacterial activity of TiO_2 - H, TiO_2- C

Bacteria	Inhibition zone in mm	
	Ab ciprofloxacin	TiO-C
Escherichia coli	22	8
Staphylococcus aureus	30	8
Bacillus subtilis	27	8
Bacillus cereus	24	9
Kleibsiella pneumonia	25	8

2) Anticorrosion Activity

The anticorrosion performance of TiO_2–C nanoparticles was evaluated in acidic, basic and neutral media. The results showed that the presence of TiO_2–C significantly reduced the corrosion rate compared to the blank sample, confirming its effective protective nature. This reduction is attributed to the formation of a stable barrier layer on the metal surface, which minimizes direct contact between the corrosive medium and the metal. In acidic medium, TiO_2–C exhibited a corrosion rate of 4.4% with an anticorrosion efficiency of 48.8%. In basic medium, the corrosion rate decreased to 4.8% with an efficiency of 31.4%, while in neutral medium, the lowest corrosion rate of 4.2% with the highest efficiency of 50.5% was observed. Overall, TiO_2–C nanoparticles demonstrated effective corrosion inhibition in all media, indicating their strong protective ability and potential application in corrosion-resistant coatings.

Table 4.3 Anticorrosion activity in Acidic Medium

Medium	W_1	W_2	ΔW (g)	Corrosion rate % $\left[\frac{W_1 - W_2}{W_1}\right] \times 100$	Anticorrosion activity in percentage (%) $\left[\frac{CR_b - CR_n}{CR_b}\right] \times 100$
Blank	1.4841	1.3341	0.1280	8.6	-
$TiO_2 - C$	1.5206	1.4732	0.0674	4.4	48.8

Table 4.4 Anticorrosion activity in Basic Medium

Medium	W_1	W_2	ΔW (g)	Corrosion rate % $\left[\frac{W_1 - W_2}{W_1}\right] \times 100$	Anticorrosion activity in percentage (%) $\left[\frac{CR_b - CR_n}{CR_b}\right] \times 100$
Blank	1.5105	1.4038	0.1067	7.0	-
$TiO_2 - C$	1.4729	1.4020	0.0709	4.8	31.4

Table 4.5 Anticorrosion activity in Neutral Medium

Medium	W_1	W_2	ΔW (g)	Corrosion rate % $\left[\frac{W_1 - W_2}{W_1}\right] \times 100$	Anticorrosion activity in percentage (%) $\left[\frac{CR_b - CR_n}{CR_b}\right] \times 100$
Blank	1.4677	1.3422	0.1255	8.5	-
TiO_2 - C	1.4473	1.3861	0.0612	4.2	50.5

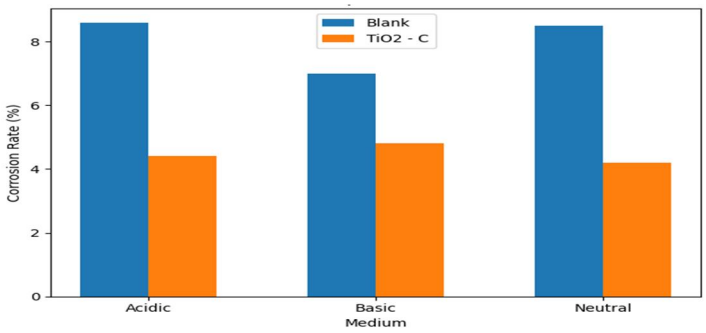

Fig. 4.10 Comparison of corrosion rate (%) in different media

3) Shelf-Life extension study of Fruits and Vegetables using Chamaecostus cuspidatus Leaf extract coating

The shelf-life extension study of capsicum, grapes and banana was carried out for five days under ambient storage conditions to evaluate the effectiveness of the *Chamaecostus cuspidatus* leaf extract coating.

ISSN: 2321-9653; IC Value: 45.98; SJ Impact Factor: 7.538
Volume 14 Issue III Mar 2026- Available at www.ijraset.com

In capsicum coated and uncoated samples appeared fresh with natural colour and firm texture on Day 1 and Day 2, as shown (Fig. 4.11). By Day 3, the uncoated capsicum started showing slight shrinkage and loss of surface gloss, indicating the beginning of moisture loss, while the coated sample retained better firmness and maintained its natural green colour. On Day 4, the uncoated capsicum exhibited noticeable deterioration such as increased shrinkage and slight discoloration, whereas the coated capsicum still maintained comparatively good appearance and texture. By Day 5, the uncoated capsicum showed clear signs of spoilage and severe surface shrinkage, while the coated sample continued to retain relatively better colour, firmness and overall visual quality.

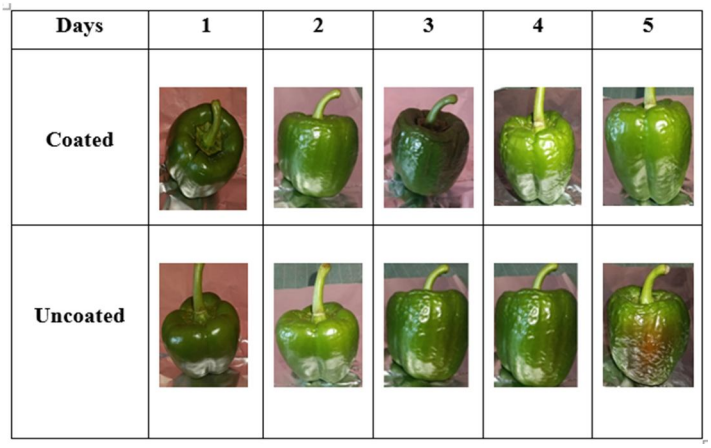

Fig. 4.11 Shelf-Life Extension Study of Capsicum

In grapes (Fig. 4.12), both coated and uncoated samples appeared fresh with natural colour and intact clustered structure on Day 1 and Day 2. On Day 3, the coated grapes maintained their freshness with minimal dehydration, whereas the uncoated grapes began to show slight shriveling. By Day 4, the uncoated grapes exhibited increased dehydration and early signs of deterioration, while the coated grapes still retained better colour and structure. On Day 5, severe dehydration and visible microbial spoilage were observed in the uncoated grapes, whereas the coated grapes maintained comparatively better freshness and appearance.

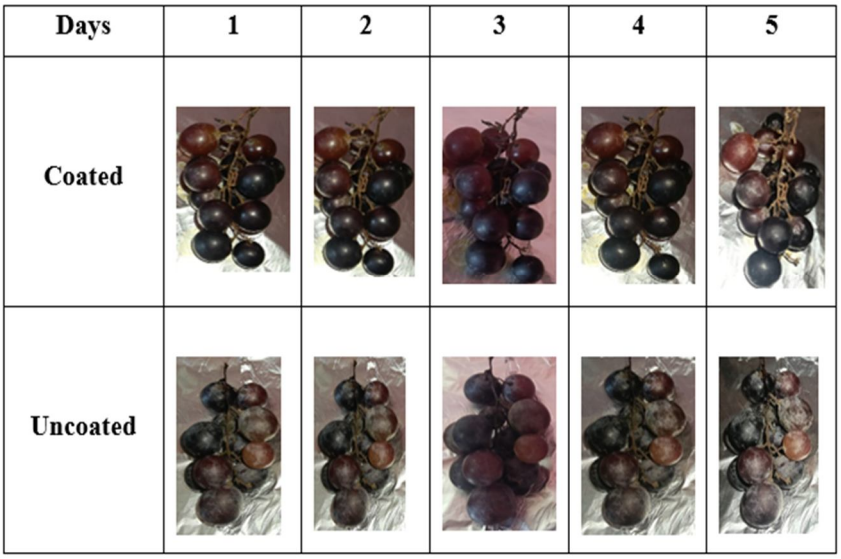

Fig. 4.12 Shelf-Life Extension Study of Grapes

In banana (Fig. 4.13), both samples appeared fresh on Day 1 and Day 2. By Day 3, brown spots began to appear more prominently on the uncoated banana, indicating faster ripening. On Day 4 and Day 5, the uncoated banana showed extensive browning and over-ripening, while the coated banana exhibited comparatively delayed ripening with fewer dark spots and better firmness. The improved storage stability of the coated samples may be attributed to the formation of a thin protective layer produced by the *Chamaecostus cuspidatus* extract, which likely reduced moisture loss, respiration rate and microbial growth.

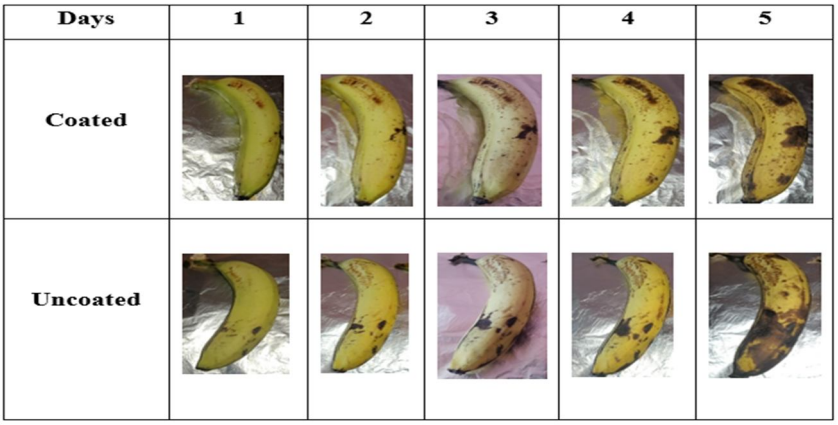

Fig. 4.13 Shelf-Life Extension Study of Banana

Overall, the coated samples demonstrated better preservation of visual quality and extended shelf life compared to the uncoated samples.

V. CONCLUSION

Green synthesis of nanoparticles using plant extracts has gained considerable attention due to its eco-friendly, cost-effective and sustainable approach. The present study successfully demonstrated the synthesis of TiO_2 nanoparticles using *Chamaecostus cuspidatus* leaf extract (TiO_2–C) as a green reducing and stabilizing agent. The synthesized nanoparticles were characterized using various analytical techniques and evaluated for antibacterial, anticorrosion and shelf-life extension applications.

The UV–Visible spectrum showed an absorption peak at 286 nm, confirming the formation of nanosized TiO_2 with semiconducting behaviour. FT-IR analysis revealed O–H, C–H and Ti–O–Ti vibrations, indicating the involvement of phytochemicals in reduction and stabilization. XRD results confirmed the anatase phase with characteristic diffraction peaks and an average crystallite size of 12.10 nm. FE-SEM analysis showed agglomerated quasi-spherical nanoparticles with an average size of ~85 nm, while EDAX confirmed the presence of titanium and oxygen with good purity. Thermal analysis indicated good stability with a final residue of 89.7%, confirming the formation of stable TiO_2 at higher temperatures.

The antibacterial study demonstrated moderate activity against *Escherichia coli*, *Staphylococcus aureus*, *Bacillus subtilis*, *Bacillus cereus* and *Klebsiella pneumoniae*. Anticorrosion studies revealed that TiO_2–C significantly reduced corrosion rates to 4.4%, 4.8% and 4.2% in acidic, basic and neutral media, respectively, compared to higher corrosion in the unmodified sample. The highest corrosion was observed in acidic medium and lowest in neutral medium. Furthermore, shelf-life studies showed that treated fruits and vegetables retained better color, firmness and overall quality compared to untreated samples.

Overall, the results confirm that TiO_2–C nanoparticles possess good crystallinity, thermal stability, antibacterial activity, corrosion resistance and preservation ability, making them a promising eco-friendly multifunctional material for various applications.

VI. ACKNOWLEDGMENT

I would like to express my gratitude to my primary supervisor Dr. J. Antony Rajam., who guided me throughout this research article. I would also like to thank my friends and family who supported me and offered deep insight into the study.

REFERENCES

[1] Nath Dand Banerjee P., “Green nanotechnology- a new hope for medical biology” Environmental Toxicol Pharmacol, 36, 997–1014, https://doi.org/10.1016/j.etap. 09.002.
[2] BPoizot P., Laruelle S., Grugeon S., Dupont L. and Tarascon J. M., “Nano-sized transition-metal oxides and negative-electrode materials for lithium-ion batteries” Nature, 407, 496–499, https://doi.org/10.1038/35035045.
[3] Nyamukamba, P., Okoh, O., Mungondori, H., Taziwa, R., Zinya, S., “Synthetic methods for titanium dioxide nanoparticles: a review. In: Yang, D. (Ed.), Titanium Dioxide—Material for a Sustainable Environment” 151.
[4] Kshtriya, B. Koshti, N. Gour., “Green synthesized nanoparticles: Classification, synthesis, characterization and applications, in: Comprehensive Analytical Chemistry” 94, Elsevier, 173–222, https://doi.org/10.1016/bs.coac.2020.12.009.
[5] Sakshi Sikaria, Shivalingam Chitra, Ramasamy Ramasubburayan., “Vitex negundo leaf extract-assisted synthesis of TiO_2 nanoparticles and deciphering its in vitro antibacterial, antibiofilm, cytotoxic and anti-migratory activities” Materials Letters, 403, 139460, https://doi.org/10.1016/j.matlet.2025.139460.

[6] Abouelkacem Sahraoui, Mouna Hamlaoui, Sara chichi, "Green synthesis and characterization of titanium dioxide nanoparticles using Eucalyptus globulus leaf extract: Impacts of the mild thermal treatment" Materials Today Sustainability. https://doi.org/10.1016/j.mtsust.2025.101193.

[7] Khrsheed Ahmed, Pooja Singh, SurendraK. Yadav, Arvind Kumar, SheoK. Mishra, Jay Singh., "Highly precise electrochemical biosensing of urea through Trigonella foenum-graecum leaf extract mediated green synthesis of titanium dioxide nanoparticles" Inorganic chemistry communications, 176, 114151, https://doi.org/10.1016/j.inoche.2025.114151.

[8] Aminur Rahman et al., "Green synthesis of antibacterial TiO_2 nanoparticles using citrus lemon extract to combat MDR Clostridium perfringens" Environmental Technology & Innovation, 39, 104347, https://doi.org/10.1016/j.eti.2025.104347.

[9] Shinta, Adelia Oktaviana, Chika, Eka Nurfani, Evi Maryanti, Dicky Annas, Muhamad Nikmatullah, Dewangga Oky Bagus Apriandanu, Iwan Syahjoko Saputra., "Effect of Elaeis guineensis Jacq. Leaf extracts concentration in the optical, structure, morphology analysis of titanium dioxide nanoparticles" Results in Surfaces and Interfaces, 18, 100391, https://doi.org/10.1016/j.rsurfi.2024.100391.

[10] S. Shanavas, A. Priyadharsan, S. Karthikeyan, K. Dharmaboopathi, I. Ragavan, C. Vidya, R. Acevedo, P.M. Anbarasana., "Green synthesis of titanium dioxide nanoparticles using Phyllanthus niruri leaf extract and study on its structural, optical and morphological properties" Materials today proceedings, 26, 4, 3531-3534, https://doi.org/10.1016/j.matpr.2019.06.715.

[11] Mohammad Zaki Ahmad et al., "Green Synthesis of Titanium Dioxide Nanoparticles Using Ocimum sanctum Leaf Extract: In Vitro Characterization and Its Healing Efficacy in Diabetic Wounds" 27, 7712. https://doi.org/10.3390/molecules27227712.

[12] M. Aravind et al., (2021) "Synthesis of TiO_2 nanoparticles by chemical and green synthesis methods and their multifaceted properties" SN Applied Sciences, 3, 409, https://doi.org/10.1007/s42452-021-04281-5.

[13] Parker R L, "Zur Kristallstruktur von Anastas und Rutil. (II. Teil. Die Anastasstruktur).", Zeitschrift fuer Kristallographie, Kristallgeometrie, Kristallphysik, Kristallchemie (-144,1977) 59, 1-54 (1924) (*)2theta values have been shifted internally for the calculation of the amounts, the intensity scaling factors as well as the figure-of-merit (FoM), due to the active search-match option 'Automatic zero-point adaption'.

[14] Hanaor, D. A. H., & Sorrell, C. C., "Review of the anatase to rutile phase transformation" Journal of Materials Science, 46(4), 855–874. https://doi.org/10.1007/s10853-010-5113-0

[15] Chen, X., & Mao, S. S. (2007) "Titanium dioxide nanomaterials: Synthesis, properties and applications" Chemical Reviews, 107(7), 2891–2959. https://doi.org/10.1021/cr0500535

[16] Nisha Elizabeth Sunny, Sneha Susan Mathew, Nandita Chandel, Panchamoorthy Saranavan, R. Rajeshkannan, M. Rajasimman, Yasser Vasseghian, N. Rajamohan, "Green synthesis of titanium dioxide nanoparticles using plant biomass and their applications- A review" Chemosphere, 300, 134612, https://doi.org/10.1016/j.chemosphere.2022.134612.

[17] S. Pavithra, T.C. Bessy, M.R. Bindhu, Ragavendran Venkatesan, R. Parimaladevi, Mohammed Mujahid Alam, Jeyanthinath Mayandi, M. Umadevi., "Photocatalytic and photovoltaic applications of green synthesized titanium oxide (TiO_2) nanoparticles by Calotropis gigantea extract" Journal of Alloys and Compounds, 960, 170638, https://doi.org/10.1016/j.jallcom.2023.170638.

[18] Diana Rakhmawaty Eddy, Devi Rahmawati, Muhamad Diki Permana, Takahiro Takeri, Solihudin, Atiek Rostika Noviyanti, Iman Rhayu., "A review of recent developments in green synthesis of TiO_2 nanoparticles using plant extract: Synthesis, characterization and photocatalytic activity" Inorganic Chemistry Communications, 165, 112531, https://doi.org/10.1016/j.inoche.2024.112531.

[19] Kirby, W.M.M., Bauer, A.W., Sherris, J.C., Turck, M. (1966). Antibiotic susceptibility testing by a standardized single disk method. American Journal of Clinical Pathology, 45(4), 493–496.

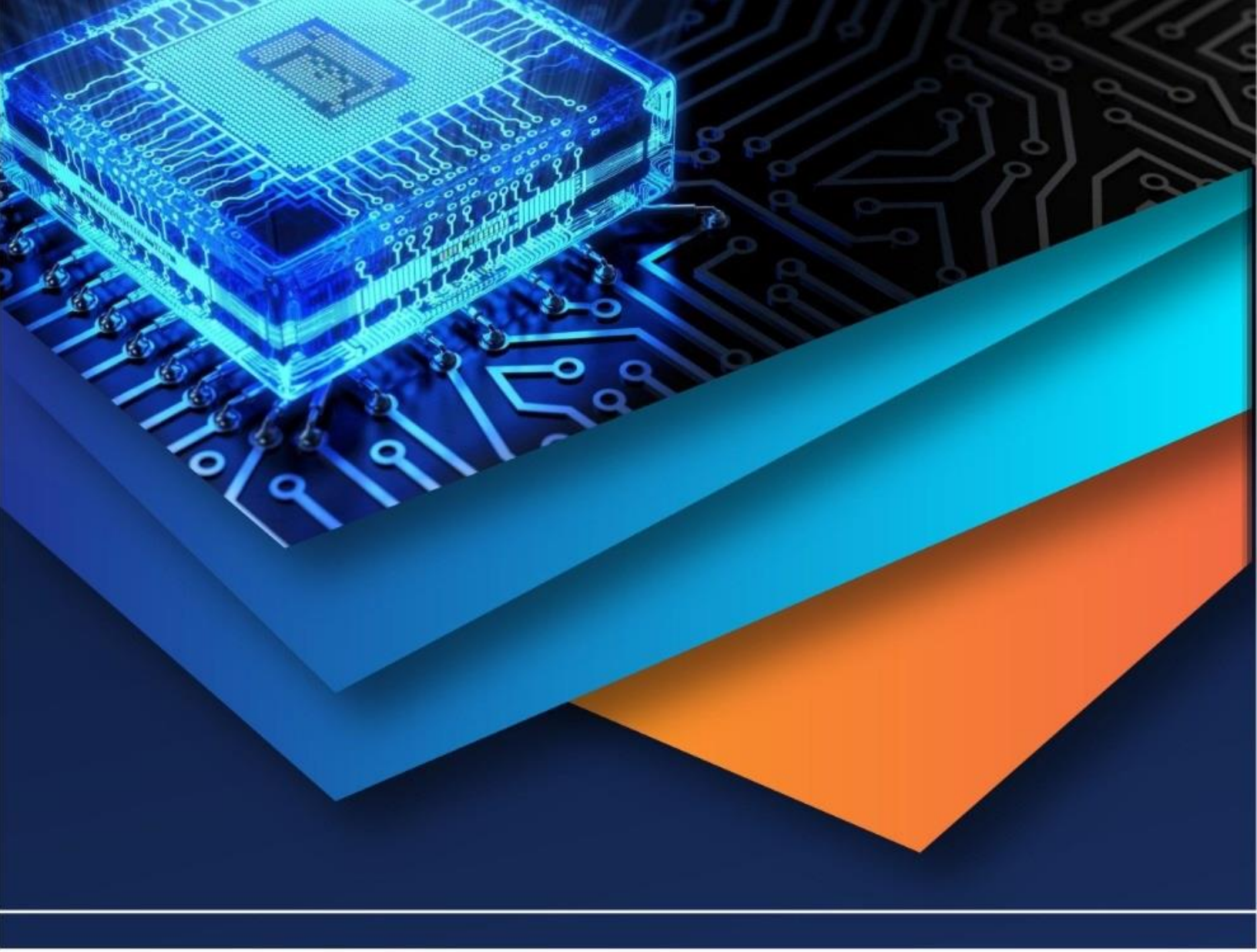

10.22214/IJRASET

45.98

IMPACT FACTOR: 7.129

IMPACT FACTOR: 7.429

INTERNATIONAL JOURNAL FOR RESEARCH

IN APPLIED SCIENCE & ENGINEERING TECHNOLOGY